The 9th European Congress on Computational Methods in Applied Sciences and Engineering
ECCOMAS Congress 2024
3–7 June 2024, Lisboa, Portugal

LIMIT ANALYSIS OF MASONRY STRUCTURES: UPPER BOUND APPROACH BASED ON HOMOGENIZATION AND LOCAL MESH REFINEMENT

NICOLA GRILLANDA[1] AND VINCENZO MALLARDO[2]

[1] Department of Architecture
University of Ferrara
Via Quartieri 8, 44121 Ferrara, Italy
e-mail: nicola.grillanda@unife.it

Department of Architecture
University of Ferrara
Via Quartieri 8, 44121 Ferrara, Italy
e-mail: vincenzo.mallardo@unife.it

Key words: Upper bound limit analysis, Masonry structures, Homogenization, Local mesh refinement

Summary. We present an upper bound limit analysis tool for plane stress problems in masonry. A given masonry construction is discretized into planar rigid-perfectly plastic finite elements, whose kinematics is described by rigid body velocities and plastic strain rates. To properly represent the collapse behaviour of the heterogeneous masonry material, the plastic strain rates must follow the homogenized kinematic conditions derived for running bond masonry textures. For a given load configuration, a rigid-plastic limit analysis problem can be defined and solved to find a mechanism and an associated collapse load. Local mesh refinement is finally applied to optimize the representation of the mechanism and minimize the collapse load.

1 INTRODUCTION

Masonry structures constitute a large part of the historical heritage. The interest in developing new computational tools for the study and the preservation of such constructions is still high [1, 2, 3] and several numerical tools have been proposed during the years [4, 5, 6]. After recent earthquakes, the interest in computational tools that can efficiently reproduce the collapse behaviour of masonry structures, such as limit analysis methods based on the kinematic theorem, has increased [7, 8].

Any numerical method conceived to assess masonry constructions must take into account the main non-linearities of masonry, which are negligible elastic deformation, almost null resistance in tension compared with a good compressive strength and shear strength [9]. Limit analysis tools are often applied by idealizing masonry as a no-tension material, in agreement with Heyman's studies (1969) [10]. Later, some heterogeneous limit analysis methods were presented. In these approaches, each brick composing the masonry material is modeled as an independent element and mortar joints are reduced to frictional zero-thickness interfaces. Such strategy is popular, since it allows an accurate reproduction of the structural behaviour, see [11, 12]. Otherwise, homogenization-based methods were presented to avoid the heterogeneous modelling strategy [13, 14, 15]. Homogenization allows representing masonry as an equivalent homogeneous material, where all potential failure modes are represented with respect of the associated flow rule. The use of homogenization can be advantageous, since it allows for computationally cheap models even in case of complex and large structures maintaining the reliability of the obtained results.

What is presented in this work is an upper bound limit analysis model for plane-stress masonry problems. This is obtained from the conjunction of homogenization theory by de Buhan & de Felice [16], rigid-plastic limit analysis [17], and a local mesh refinement strategy. Once defined a discretization into triangular finite elements for a given structure, the kinematics of each element is described by rigid body velocities and plastic strain rates. Plastic strain rates must satisfy homogenized kinematic conditions derived from the application of associative flow rule to the reference volume element (RVE): this ensure that the actual masonry texture is properly taken into account. Then, an upper bound limit analysis problem is formulated in agreement with the kinematic theorem of limit analysis. Finally, a local mesh refinement strategy is applied to optimize the mechanism representation and minimize any intrinsic overestimation of the collapse load. The theoretical formulation is here presented, together with a simple numerical application.

2 HOMOGENIZATION MODEL

By following the classic homogenization model proposed by de Buhan & de Felice [16] for single-leaf running bond masonry, the representative volume element (RVE) can be identified by simply considering four adjacent bricks. Each brick is assumed as a rigid and infinitely resistant block. Mortar joints are reduced to zero-thickness frictional interfaces. This allows describing the kinematics of the RVE through 4 parameters only, i.e. the three strain rates constituting the 2D strain rate tensor ($\epsilon_{11}, \epsilon_{22}, \epsilon_{12}$) and the in-plane rotation rate ω_3. A graphic representation of the contribution of each strain rate on the RVE is depicted in Figure 1.

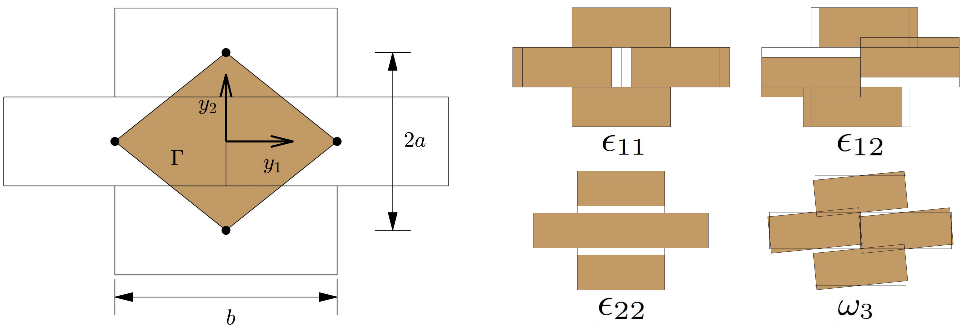

Figure 1: Reference volume element (RVE) and graphic representation of strains rates.

The kinematics of any point $P : \mathbf{y}^P = \left[y_1^P, y_2^P\right]^{\mathrm{T}}$ belonging to the brick having centroid $G : \mathbf{y}^G = \left[y_1^G, y_2^G\right]^{\mathrm{T}}$ can be expressed as:

$$\mathbf{v}^{G\rightarrow P} = \mathbf{E}\mathbf{y}^G + \boldsymbol{\Omega}\left(\mathbf{y}^P - \mathbf{y}^G\right), \text{ where } \mathbf{E} = \begin{bmatrix} \epsilon_{11} & \epsilon_{12} \\ \epsilon_{12} & \epsilon_{22} \end{bmatrix}, \boldsymbol{\Omega} = \begin{bmatrix} 0 & -\omega_3 \\ \omega_3 & 0 \end{bmatrix} \tag{1}$$

Eq 1 can be easily used to compute the velocity jump along the joints. Considering for instance the j-th joint belonging to the boundary of the i-th and the k-th brick, the velocity jump is constant along the joint and is computed as:

$$\Delta \mathbf{v}^{\mathrm{j}} = \mathbf{v}^{G_{\mathrm{i}}\rightarrow P} - \mathbf{v}^{G_{\mathrm{k}}\rightarrow P} = (\mathbf{E} - \mathbf{\Omega})\left(\mathbf{y}^{G_{\mathrm{i}}} - \mathbf{y}^{G_{\mathrm{k}}}\right) \tag{2}$$

The velocity jumps along all the joints must respect the flow rule imposed in agreement with the Mohr-Coulomb frictional behaviour. Therefore, it must be imposed that:

$$\Delta v_n^{\mathrm{j}} \geq \mu \left|\Delta v_s^{\mathrm{j}}\right|, \text{ for j} = 1...5 \tag{3}$$

where μ is the friction coefficient, Δv_n^{j} and Δv_s^{j} denote the normal and tangential component of the velocity jump. By expressing Eq 3 in terms of strain rates, the following inequalities are obtained:

$$\frac{\mu}{2}\,\left|2\,\epsilon_{12} - \epsilon_{11}\,\beta + 2\,\omega_3\right| \leq \epsilon_{22} - \frac{\epsilon_{12}\,\beta}{2} + \frac{\omega_3\,\beta}{2} \tag{4a}$$

$$\frac{\mu}{2}\,\left|2\,\epsilon_{12} + \epsilon_{11}\,\beta + 2\,\omega_3\right| \leq \epsilon_{22} + \frac{\epsilon_{12}\,\beta}{2} - \frac{\omega_3\,\beta}{2} \tag{4b}$$

$$\mu\,\left|\epsilon_{12} - \omega_3\right| \leq \epsilon_{11} \tag{4c}$$

where β is the basis-height ratio of the brick. Eqs 4 constitute the plastic flow rule expressed in terms of plastic strain rates, thus suitable for application in the limit analysis of a rigid-plastic homogeneous material equivalent to masonry. In turn, the internal power per unit area can be derived as follows:

$$\mathcal{P}_{\mathrm{int}}^{\Gamma} = \frac{t}{ab}\sum_{\mathrm{j}=1}^{5} c\left|\Delta v_s^{\mathrm{j}}\right| = \frac{t}{ab}\sum_{\mathrm{j}=1}^{5} c\frac{\Delta v_n^{\mathrm{j}}}{\mu} = \frac{ct\,(\epsilon_{11} + \epsilon_{22})}{\mu} \tag{5}$$

where t is the thickness of the bricks and c is the cohesion. It can be observed that the internal power does not depend on the shear strain rate ϵ_{12}. Note also that for the case of dry joints masonry the internal power is null.

3 LIMIT ANALYSIS FORMULATION

We can consider now a planar domain $\mathcal{D} \in \mathbb{R}^2$ in the reference system Ox_1x_2. A discretization into N triangular finite elements is performed: each element is a constant strain element with rigid-perfectly plastic behaviour. Therefore, the degrees of freedom associated to the i-th element having centroid $G_{\mathrm{i}} : \mathbf{x}^{G_{\mathrm{i}}} = [x_1^{G_{\mathrm{i}}}, x_2^{G_{\mathrm{i}}}]^{\mathrm{T}}$ are the translational rigid velocities of the centroid $\mathbf{v}^{G_{\mathrm{i}}} = [v_1^{G_{\mathrm{i}}}, v_2^{G_{\mathrm{i}}}]^{\mathrm{T}}$, the in-plane rigid rotation ϕ_3^{i}, the plastic strain rates $\boldsymbol{\epsilon}^{\mathrm{i}} = [\epsilon_{11}^{\mathrm{i}}, \epsilon_{22}^{\mathrm{i}}, \epsilon_{12}^{\mathrm{i}}]^{\mathrm{T}}$ and the plastic micro-rotation ω_3^{i}. The kinematics of any point $P : \mathbf{x}^P = [x_1^P, x_2^P]^{\mathrm{T}}$ belonging to the i-th element is therefore expressed as follows:

$$\mathbf{v}^{G_{\mathrm{i}}\rightarrow P_{\mathrm{j}}} = \mathbf{v}^{G_{\mathrm{i}}} + \mathbf{\Omega}^{\mathrm{i}}\left(\mathbf{x}^{P_{\mathrm{j}}} - \mathbf{x}^{G_{\mathrm{i}}}\right) + \mathbf{E}^{\mathrm{i}}\left(\mathbf{x}^{P_{\mathrm{j}}} - \mathbf{x}^{G_{\mathrm{i}}}\right) \tag{6}$$

where $\mathbf{E}^{\mathrm{i}}$ and $\mathbf{\Omega}^{\mathrm{i}}$ are the strain rates tensor and rotation tensor for the i-th element.

Having maintained the assumption of small displacements, the element kinematics is expressed as linear combination between the degrees of freedom. This allows to express the overall kinematic limit analysis problem as a linear programming (LP) problem. By assembling the degrees of freedom of the N elements in the global vectors $\mathbf{v}$, $\boldsymbol{\phi}$, $\boldsymbol{\epsilon}$, $\boldsymbol{\omega}$, the following LP problem can be formulated:

$$
\begin{aligned}
\text{minimize} \quad & \lambda = -\mathbf{f}_{\mathrm{D}}^{\mathrm{T}} \begin{bmatrix} \mathbf{v} & \boldsymbol{\phi} & \boldsymbol{\epsilon} \end{bmatrix}^{\mathrm{T}} + \mathbf{w}^{\mathrm{T}} \boldsymbol{\epsilon} && \text{(7a)} \\
\text{subject to} \quad & \mathbf{C} \begin{bmatrix} \mathbf{v} & \boldsymbol{\phi} & \boldsymbol{\epsilon} \end{bmatrix}^{\mathrm{T}} = \mathbf{0} && \text{(7b)} \\
& \mathbf{A}_{\mathrm{fix}} \begin{bmatrix} \mathbf{v} & \boldsymbol{\phi} & \boldsymbol{\epsilon} \end{bmatrix}^{\mathrm{T}} = \mathbf{0} && \text{(7c)} \\
& \mathbf{P} \begin{bmatrix} \boldsymbol{\epsilon} & \boldsymbol{\omega} \end{bmatrix}^{\mathrm{T}} \leq \mathbf{0} && \text{(7d)} \\
& \mathbf{f}_{\mathrm{L}}^{\mathrm{T}} \begin{bmatrix} \mathbf{v} & \boldsymbol{\phi} & \boldsymbol{\epsilon} \end{bmatrix}^{\mathrm{T}} = 1 && \text{(7e)}
\end{aligned}
$$

where λ is the load factor, $\mathbf{f}_{\mathrm{D}}$ is the vector of permanent loads (dead loads) and $\mathbf{f}_{\mathrm{L}}$ is the vector of the loads which depend on λ (live loads), and finally $\mathbf{w}$ is the internal power vector. Within the problem 7, 7a is the objective function obtained by applying the principle of virtual powers, 7b are the node compatibility constraints, 7c are the geometric constraints, 7d is the plastic flow rule obtained by expressing Eq 4 in matrix form, and 7e is the normalization of the power associated to live loads.

The LP problem 7 can be easily solved by using modern optimization software, such as MOSEK [18], and provides a load factor and an associated mechanism, the latter composed of rigid body motion and plastic strain rates.

4 LOCAL MESH REFINEMENT

According to the kinematic theorem of limit analysis, the load factor obtained from 7 constitutes an upper bound of the actual collapse load. The overestimation of the load-bearing capacity is also affected by the adopted mesh, since the plastic strain rates are constant within the element. To reduce such mesh dependencies, a local mesh refinement procedure is followed.

The procedure is simple. Once the LP problem has been solved for the initial mesh and a first load factor has been found, the mesh is refined only in the regions presenting plastic strain rates. In other words, elements presenting only rigid body motion do not require any refinement. A criterion based on the $\mathbb{L}_2$-norm of plastic strain rates is used to automatically drive the refinement. In particular, the i-th element is refined into 4 new triangular elements having equal area only if the following condition is satisfied:

$$\eta^{\mathrm{i}} \geq \xi \sum_{\mathrm{j}=1}^{N} \eta^{\mathrm{j}} \tag{8}$$

where ξ is a tolerance parameter and η is the $\mathbb{L}_2$-norm of plastic strain rates so defined:

$$\eta^{\mathrm{i}} = A_{\mathrm{i}} \left|\left|\boldsymbol{\epsilon}^{\mathrm{i}}\right|\right| \tag{9}$$

where A_{i} is the area of the element. Moreover, to avoid hanging nodes in the refined mesh, elements adjacent to those satisfying Eq 8 must be also subdivided accordingly.

This procedure allows to easily built a new mesh with higher density in the plasticized regions. The LP problem can be defined again considering the new mesh and another load factor is computed. The local mesh refinement is iteratively applied until the convergence of the load factors is found.

5 APPLICATION TO A SQUARE WALL

The presented homogenized rigid-plastic limit analysis is now applied to a simple numerical example regarding a square wall fixed at the bottom edge and subjected to in-plane horizontal load. Such example was first proposed in [19] and then analysed in [20] via associative and non-associative limit analysis. The wall is composed of running bond masonry texture with bricks having basis-height ratio equal to 3: a total of 48 rows has been considered. The live load condition is a horizontal load proportional to the self-weight. The friction coefficient is equal to 0.75 whereas cohesion is assumed null, thus representing a dry joints masonry. In this way, the load factor is not affected by thickness and unit weight of the material. The load factors obtained in [20] via associated and non-associated limit analysis were equal to 0.5450 and 0.5396 respectively. Such example is here studied by means of the proposed approach. Results have been compared with those published in [20] in terms of load factor and mechanism, see Figure 2.

By comparing the homogenized rigid-plastic outcome from iteration 0, i.e. initial mesh, to iteration 4, refined mesh, it is evident that load factor and the corresponding mechanism suffer some mesh dependency effects that can be minimized through local mesh refinement. The load factor associated to the initial mesh is equal to 0.6148, which is 12.7% higher than the value obtained via associative rigid block limit analysis. On the contrary, a 0.5034 load factor has been found after mesh refinement. Such value is 6.7% lower than the one obtained via non-associative rigid block limit analysis. Also, the solution at the last iteration was obtained in 29 seconds using a PC equipped with an Intel Core I7-1165G7 processor and 16Gb RAM. For such case, it can be stated that the collapse behaviour has been properly reproduced via the presented homogenized rigid-plastic limit analysis approach. Moreover, this approach seems able to provide conservative results even in comparison with non-associative rigid block limit analysis.

6 CONCLUSIONS

In this work, an rigid-plastic limit analysis model enriched with homogenization and local mesh refinement is presented. Homogenization is applied on the classic running bond texture to derive the kinematic conditions expressing internal power and flow rule in terms of plastic strains. A rigid-plastic limit analysis model, where each element can present rigid body motion and plastic strain rates, is then applied. Finally, the initial mesh is iteratively refined until the convergence of the load factor values is obtained. The use of homogenization allows avoiding the modelling of each element constituting the masonry material. Then, the local mesh refinement techniques permits minimizing any mesh dependency effect and reducing the overestimation of the load bearing capacity. Safe results have been obtained in comparison with traditional heterogeneous limit analysis models, including also models relying on non-associative approaches. Next applications will involve larger and geometrically more complex examples, as well as masonry composed of different textures, and extensions to fully three-dimensional approaches.

REFERENCES

[1] Mallardo, V., Malvezzi, R., Milani, E., and Milani, G. 2008. "Seismic vulnerability of historical masonry buildings: A case study in Ferrara." Eng Struct 30, no. 8: 2223–2241. https://doi.org/10.1016/j.engstruct.2007.11.006

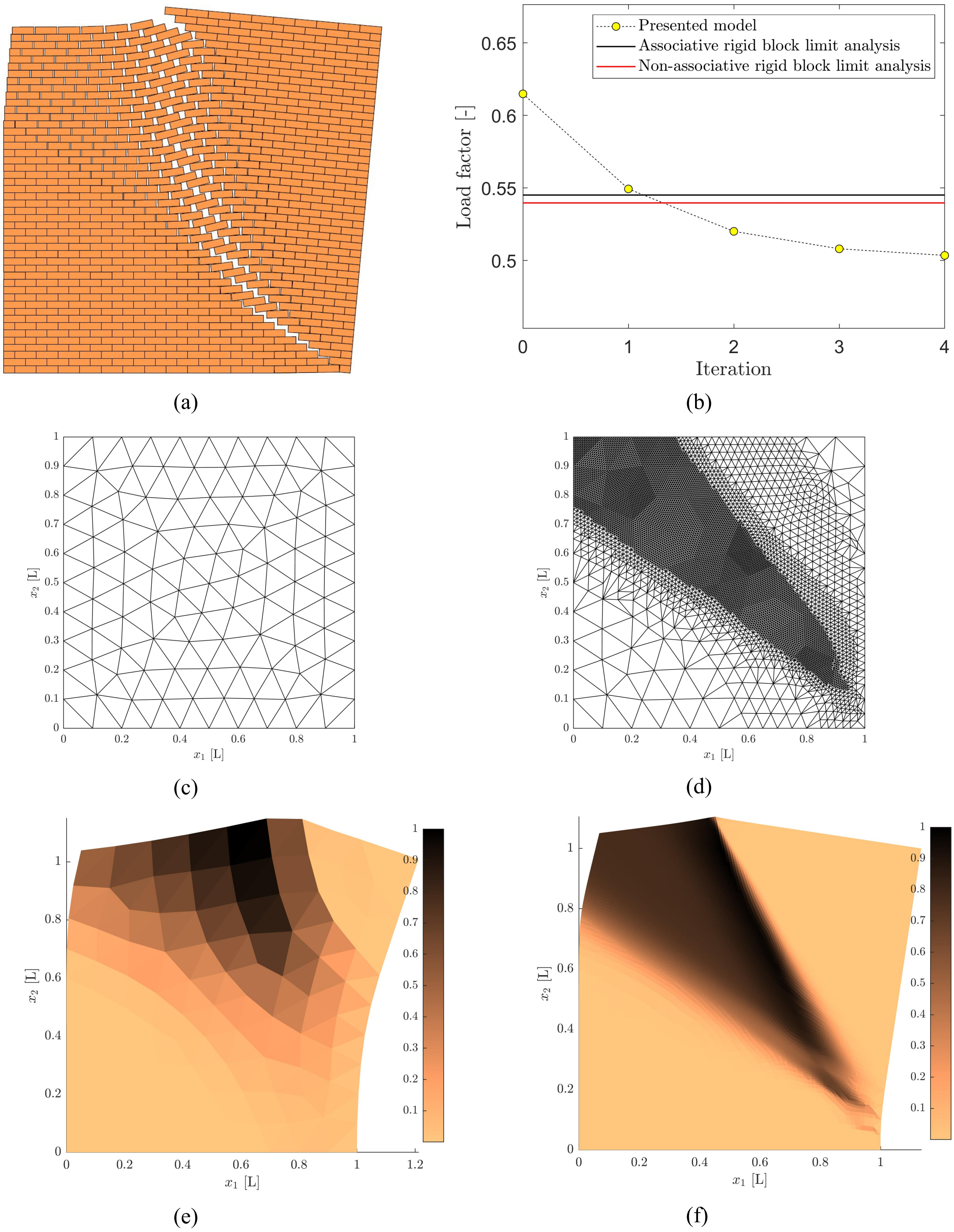

Figure 2: Lourenço wall: (a) non-associative rigid-block mechanism (from [20]), (b) comparison of load factors obtained via presented approach and rigid block limit analysis in [20], (c, d) initial and refined mesh in homogenized rigid-plastic limit analysis, (e, f) rigid plastic mechanisms with initial and refined mesh. The colour map in (e, f) denotes the normalized principal plastic strain rate.

[2] Alessandri, C., Garutti, M., Mallardo, V., and Milani, G. 2015. "Crack patterns induced by foundation settlements: integrated analysis on a renaissance masonry palace in Italy." Int J Archit Herit 9, no. 2: 111-129. https://doi.org/10.1080/15583058.2014.951795

[3] De Fabrizio, M., and Mallardo, V. 2023. "Structural analysis of masonry square vaults in the Italian region of Apulia." Buildings 13, no. 8: 1997. https://doi.org/10.3390/buildings13081997

[4] D'Altri, A. M., Sarhosis, V., Milani, G., Rots, J., Cattari, S., Lagomarsino, S., Sacco, E., Tralli, A., Castellazzi, G., and de Miranda, S. 2020. "Modeling strategies for the computational analysis of unreinforced masonry structures: review and classification." Arch Comput Methods Eng 27: 1153–1185. https://doi.org/10.1007/s11831-019-09351-x

[5] Occhipinti, G., Caliò, I., D'Altri, A. M., Grillanda, N., de Miranda, S., Milani, G., and Spacone, E. 2022. "Nonlinear finite and discrete element simulations of multi-storey masonry walls." Bullet Earthq Eng 20: 2219–2244. https://doi.org/10.1007/s10518-021-01233-7

[6] Cannizzaro, F., Castellazzi, G., Grillanda, N., Pantò, B., and Petracca, M. 2022. "Modelling the nonlinear static response of a 2-storey URM benchmark case study: comparison among different modelling strategies using two- and three-dimensional elements." Bull Earthq Eng 20: 2085–2114. https://doi.org/10.1007/s10518-021-01183-0

[7] Milani, G. 2013. "Lesson learned after the Emilia-Romagna, Italy, 20–29 May 2012 earthquakes: A limit analysis insight on three masonry churches." Eng Fail Anal 34:761-778. https://doi.org/10.1016/j.engfailanal.2013.01.001

[8] Pavlovic, M., Reccia, E., and Cecchi, A. 2016. "A procedure to investigate the collapse behavior of masonry domes: some meaningful cases." Int J Archit Herit 10, no. 1: 67-83. https://doi.org/10.1080/15583058.2014.951797

[9] Alessandri, C., and Mallardo, V. 1999. "Crack identification in two-dimensional unilateral contact mechanics with the boundary element method." Comput Mech 24, no. 2: 100-109. https://doi.org/10.1007/s004660050442

[10] Heyman, J. 1966. "The stone skeleton." Int J Solid Struct 2, no. 2: 249-279. https://doi.org/10.1016/0020-7683(66)90018-7

[11] Cascini, L., Gagliardo, R., and Portioli, F. 2020. "LiABlock 3D: a software tool for collapse mechanism analysis of historic masonry structures." Int J Archit Herit 14, no. 1: 75-94. https://doi.org/10.1080/15583058.2018.1509155

[12] Grillanda, N., Chiozzi, A., Milani, G., and Tralli, A. 2022. "NURBS solid modeling for the three- dimensional limit analysis of curved rigid block structures." Comput Methods Appl Mech Eng 399, no. 115304. https://doi.org/10.1016/j.cma.2022.115304

[13] Milani, G., Lourenço, P. B., and Tralli, A. 2006. "Homogenised limit analysis of masonry walls, Part I: Failure surfaces". Comput Struct 84, no. 3-4: 166-180. https://doi.org/10.1016/j.compstruc.2005.09.005

[14] Tiberti, S., Grillanda, N., Mallardo, V., and Milani, G. 2020. "A genetic algorithm adaptive homogeneous approach for evaluating settlement-induced cracks in masonry walls." Eng Struct 221, no. 111073. https://doi.org/10.1016/j.engstruct.2020.111073

[15] Valentino, J., Gilbert, M., Gueguin, M., and Smith, C. C. 2023. "Limit analysis of masonry walls using discontinuity layout optimization and homogenization". Int J Numer Meth Eng 124, no. 2: 358-381. https://doi.org/10.1002/nme.7124

[16] de Buhan, P., and de Felice, G. 1997. "A homogenization approach to the ultimate strength of brick masonry." J Mech Phys Solids 45, no. 7: 1085-1104. https://doi.org/10.1016/S0022-5096(97)00002-1

[17] Capsoni, A., and Corradi, L. 1997. "A finite element formulation of the rigid–plastic limit analysis problem". Int J Numer Meth Eng 40, no. 11: 2063-2086. https://doi.org/10.1002/(SICI)1097-0207(19970615)40:11<2063::AID-NME159>3.0.CO;2-%23

[18] M. ApS. 2024. The MOSEK optimization toolbox for MATLAB manual. Version 10.1. http://docs.mosek.com/latest/toolbox/index.html

[19] Orduña, A., and Lourenço, P. B. 2003. "Cap model for limit analysis and strengthening of masonry structures." J Struct Eng 129, no. 10: 1367-1375. https://doi.org/10.1061/(ASCE)0733-9445(2003)129:10(1367)

[20] Nodargi, N. A., Intriglia, C., and Bisegna, P. 2019. "A variational-based fixed-point algorithm for the limit analysis of dry-masonry block structures with non-associative coulomb friction." Int J Mech Sci 161, no. 105078. https://doi.org/10.1016/j.ijmecsci.2019.105078